MAGIC (SPECIAL) INCLINATIONS FOR FORMATION FLYING

D. Izzo[1] **and M. Sabatini**[2]

[1] *Advanced Concepts Team, European Space Agency*
[2] *Univesrity "La Sapienza", Department of Aerospace Engineering*

ABSTRACT

We investigate the possibility of obtaining periodical and pseudo-periodical relative motion between orbiting satellites. We first propose a numerical algorithm able to find pseudo-periodical solutions for any orbital environment considered. We then focus our attention to the case in which the satellites are considered in orbit around an oblate primary and we find that there exist two different couples of inclinations, (49.11^o, 130.89^o) and (63.4^o, 116.6^o), that are advantaged in allowing pseudo-periodical motion. These 'magic' inclinations (or special inclinations) represent a previously unknown feature of the geopotential field, a dynamical resonance phenomenon hidden in the description of the relative satellite motion. They can be explained in terms of relative orbit frequencies, but also analyzing the linear equations of motion representing the relative dynamics. In this last case also the inclination 67.77^o results to be special as it is found to be the only one allowing for perfectly periodical motion.

INTRODUCTION

In the year 2004 these authors, among others, started a cooperation on a project funded by the European Space Agency under the Ariadna scheme entitled "A search for invariant relative satellite motion" [1]. The project had to establish whether perfectly periodical motion was possible for the relative dynamic of satellites in orbit. The results of our effort, at that time purely numerical, were puzzling. Our calculations seemed to suggest that there was some kind of resonance phenomenon in the relative dynamics both at the classical value of 63.4^o (the critical inclination, where the absidal line rotation is cancelled completely) and at the rather peculiar value of 49.11^o that we named "*magic inclination*"(or special inclinations), as at that time we were clueless on how to explain it. Our results, summarized in [2], needed an independent confirmation before we could really rely on them. We therefore challenged the scientific community to confirm our findings and to explain them. Very recently, a group of researchers from Texas A&M University, took on the challenge and published an elegant explanation of the phenomenon [3] relating it to the matching of the relative orbit in-plane and out-of-plane frequencies. The "*magic inclinations*", suddenly, were not magic anymore. Their existence was confirmed.

The design of formation flying missions is often approached, in preliminary phases, using the Hill-Clohessey-Withshire equations (HCW) for circular orbits, or the Tschauner-Hempel equations (TH) for elliptical orbits. While this approach is in many cases valuable, its limitations appear clear whenever the formation control issue is specifically addressed [4]. The HCW and TH equations predict the existence of perfectly closed relative orbits and allow to find exact relations between the satellites relative positions and velocities, or between the relative orbital parameters that result in these types of orbits. These conditions can be used to define a reference orbit for the control system to follow. In a real case this results in a fight between the control system and all those perturbations that are not included in the TH and HCW equations, a fight that ultmately comes to the price of precious propellant mass. A different approach is to define a more accurate dynamical model, to search for an as-periodical-as-possible relative orbit and to define, starting from this, a closed orbit that preserves the useful information of the original bounded or slowly drifting orbit [5]. It is this second approach, leading to order of magnitues of fuel savings, that motivated the development of the algorithm described in [6] able to minimise the orbital drift for a given formation and that lead ultimately to the discovery of the magic inclinations. In this paper we start build on the available studies on this fascinating subject and we provide a general explanation for the magic inclinations and, in general, for the pseudo-periodicity (and periodicity) of the relative motion at a given inclination.

The paper is organized as follows. In Section 1 we describe again our algorithm to minimise the orbital drift and we present the results in the case of a formation flying around an oblate planet. In Section 2 we briefly review the explanation to the phenomenon

given by Vadali et al. [3]. We then argue that a general theoretical framework, valid also for non PCO orbitsdifferent types of orbital environments (high eccentricities and higher harmonics), is desirable and we propose a possible approach in Section 3 based on the possibility of approximating the dynamic with a linear, time-periodical system of differential equations. In section 4 we provide such a system in the case of relative motion around an oblate planet, in Section 5 we reproduce, using this system, the magic inclination phenomenon. In Section 6 we analyse the spectral properties of the linear system finding an explanation for the magic inclination and a new inclination where perfect periodical motion is possible. The following Section 7 provides a discussion on the results obtained.

1. FINDING THE MAGIC

Let the relative satellite motion dynamic be described by the differential equation $\dot{\mathbf{x}} = \mathbf{f}(\mathbf{x}, t)$. Starting from $\mathbf{x}_i$, at the time t, the system will be displaced of $\delta\mathbf{x} = \mathbf{x}_i - \mathbf{x}(t)$ from its initial state. We introduce the following optimisation problem:

$$\begin{array}{rl} \text{find:} & \mathbf{k} = [\mathbf{x}_i, t] \in \mathcal{I} \in R^7 \\ \text{to maximise:} & J(\mathbf{k}) = J(|\delta\mathbf{x}|) \\ \text{subject to:} & \dot{\mathbf{x}} = \mathbf{f}(\mathbf{x}, t) \\ & \mathbf{x}(t_i) = \mathbf{x}_i \end{array} \tag{1}$$

where the objective function J is decreasing monotonically in R^+ and has maximum value $J(0) = J_{max}$. $\mathcal{I}$ is an hyperectangle defining the search space. The solution to this problem has two main important properties: a) if the system $\dot{\mathbf{x}} = \mathbf{f}(\mathbf{x}, t)$ admits initial conditions that result in a periodical solution of period T, than these are also a solution to Eq.(1), b) if the system does not admit periodical solutions, then the solution to Eq.(1) has, at least, the minimal possible orbital drift. In this last case, if $J(\mathbf{k})$ is still J_{max}, the solution will here be called pseudo-periodical. Note that t is an optimisation variable together with the initial conditions $\mathbf{x}_i$.

In Figure 1 we report, from Sabatini et al. [2], the results obtained by solving the problem stated in Eq.(1) in the case where $\mathbf{f}(\mathbf{x}, t)$ describes the relative motion between satellites orbiting an oblate planet (only the J_2 harmonic is considered). The objective function $J(\mathbf{k})$ is defined by the expression in Eq.(2), where $J_{max} = 1000$, the search space was defined as $\mathcal{I}_1 = [-1, 1] \times [-1, 1] \times [-1, 1] \times [-5, 5]n \times [-5, 5]n \times [-5, 5]n \times [T_{kep} - 20, T_{kep} + 20]1e^{-2}$ where units are in km and sec. The optimiser used is a genetic algorithm [7] refined by a gradient method.

$$J(\mathbf{k}) = \frac{J_{max}}{1 + J_{max}\sqrt{\sum_{i=1}^{6}\left(\frac{\delta x^i}{x_0^i}\right)^2}} \tag{2}$$

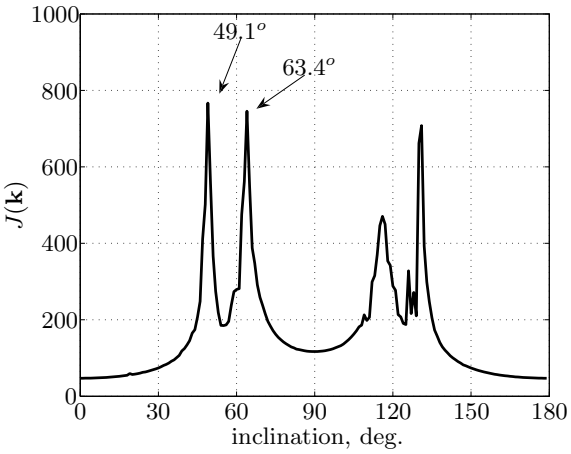

Figure 1. Resonance at the magic inclinations. (source Sabatini et al. [2])

At the two values 49.1^o and 63.4^o, and at their supplementaries, the minimal orbital drift shows an anomalous behavior. Though failing to converge perfectly to a periodical or pseudo-periodical motion ($J \neq J_{max} = 1000$), only at those inclinations the objective function climbs up to high values corresponding to a very small difference between the initial state and the state propagated for the time t.

2. EXPLAINING THE MAGIC

In this section we outline briefly the explanation of the magic inclinations given by Vadali et al. [3] making use of the vectrices notation introduced by Hughes [8]. This notation is particualrly useful here as it helps in distinguishing between vectors and their explicit representation (components) in a particular reference frame.

Consider the position vectors of two satellites $\vec{\mathbf{r}}_0$ and $\vec{\mathbf{r}}_1$. The pedices 0 and 1 refer to the chief and the deputy, to make use of a common naming in use in formation flying related literature. We define:

$$\delta\vec{\mathbf{r}} = \vec{\mathbf{r}}_1 - \vec{\mathbf{r}}_0$$

and

$$\Delta\vec{\mathbf{r}} = \frac{1}{r_1}\vec{\mathbf{r}}_1 - \frac{1}{r_0}\vec{\mathbf{r}}_0 = \hat{\mathbf{i}}_\mathbf{1} - \hat{\mathbf{i}}_\mathbf{0}$$

Introducing the vectrices $\mathcal{F}_0 = [\hat{\mathbf{i}}_\mathbf{0}, \hat{\mathbf{j}}_\mathbf{0}, \hat{\mathbf{k}}_\mathbf{0}]^T$ and $\mathcal{F}_1 = [\hat{\mathbf{i}}_\mathbf{1}, \hat{\mathbf{j}}_\mathbf{1}, \hat{\mathbf{k}}_\mathbf{1}]^T$ associated to the LHLV frames of the chief and of the deputy, we can write the last definition as:

$$\Delta\vec{\mathbf{r}} = \mathcal{F}_0^T\Delta\mathbf{r} = \mathcal{F}_0^T\begin{bmatrix}\Delta x\\ \Delta y\\ \Delta z\end{bmatrix} = \mathcal{F}_1^T\begin{bmatrix}1\\0\\0\end{bmatrix} - \mathcal{F}_0^T\begin{bmatrix}1\\0\\0\end{bmatrix}$$

and, premultiplying by $\mathcal{F}_0$ we get:

$$\Delta\mathbf{r} = \begin{bmatrix} \Delta x \\ \Delta y \\ \Delta z \end{bmatrix} = (\mathbf{C}_{01} - \mathbf{I}) \begin{bmatrix} 1 \\ 0 \\ 0 \end{bmatrix} \tag{3}$$

where $\mathbf{C}_{01} = \mathcal{F}_0 \cdot \mathcal{F}_1^T$.

Similarly we also have:

$$\delta\mathbf{r} = \begin{bmatrix} \delta x \\ \delta y \\ \delta z \end{bmatrix} = (\mathbf{C}_{01} r_1 - \mathbf{I} r_0) \begin{bmatrix} 1 \\ 0 \\ 0 \end{bmatrix}$$

the link between the unit sphere projection and the relative satellite is thus given by:

$$\begin{bmatrix} \delta x \\ \delta y \\ \delta z \end{bmatrix} = r_1 \Delta\mathbf{r} + (r_1 - r_0) \begin{bmatrix} 1 \\ 0 \\ 0 \end{bmatrix}$$

From Eq.(3) we observe that the relative motion of satellites projected on the unit sphere is uniquely determined by the rotation matrix $\mathbf{C}_{01}$ between the LHLV frames of the Chief and of the Deputy satellites. In this way relative satellite motion is mapped into rigid body motion. The rotation matrix $\mathbf{C}_{01}$, according to Euler theorem, admits the unique representation $\mathbf{C}_{01} = \exp(\mathbf{a}^\times \varphi)$, where we have introduced the rotation axis $\mathbf{a}$ and the rotation magnitude φ. We also make use of the notation $\mathbf{a}^\times$ to denote the skew matrix. We may thus represent the relative motion projection on a unit sphere as:

$$\begin{bmatrix} \Delta x \\ \Delta y \\ \Delta z \end{bmatrix} = \big(\exp(\mathbf{a}^\times \varphi) - \mathbf{I}\big) \begin{bmatrix} 1 \\ 0 \\ 0 \end{bmatrix}$$

Note that if the Deputy and the Chief are not too far apart the rotation between the two LHLV frames is very small, as a consequence $\varphi << 1$ and $\exp(\mathbf{a}^\times \varphi) = \mathbf{I} + \mathbf{a}^\times \varphi$. We may write:

$$\begin{bmatrix} \Delta x \\ \Delta y \\ \Delta z \end{bmatrix} = \mathbf{a}^\times \varphi \begin{bmatrix} 1 \\ 0 \\ 0 \end{bmatrix} = 2\epsilon^\times \begin{bmatrix} 1 \\ 0 \\ 0 \end{bmatrix}$$

or, equivalently:

$$\Delta\mathbf{r} = 2\epsilon^\times \hat{\mathbf{i}} \tag{4}$$

where we have introduced the Euler parameters ϵ describing $\mathbf{C}_{01}$. In close proximity formation flying, (defined by the condition $\varphi << 1$), we may therefore affirm that the Euler parameters ϵ representing the orientation of LHLV frame of the deputy with respect to the LHLV frame of the chief are linearly related to cartesian description of the relative satellite motion projected on a unit sphere. Using the relations between Euler parameters and Euler angles it is not difficult to show that from Eq.(4) we get directly:

$$\begin{aligned} \Delta x &= 0 \\ \Delta y &= \Delta\theta + \cos i_0 \Delta\Omega \\ \Delta z &= -\cos\theta_0 \sin i_0 \Delta\Omega + \sin\theta_0 \Delta i \end{aligned}$$

and thus:

$$\begin{aligned} \delta x &= r_1 - r_0 \\ \delta y &= r_1(\Delta\theta + \cos i_0 \Delta\Omega) \\ \delta z &= r_1(-\cos\theta_0 \sin i_0 \Delta\Omega + \sin\theta_0 \Delta i) \end{aligned} \tag{5}$$

where θ, Ω, i represent the argument of latitude, the longitude of the ascending node and the inclination. Vadali et al. [3] start from these linearised equations and evaluate, under the assumption of small eccentricities, the fundamental frequencies n_{xy} and n_z of the in plane motion (x, y) and of the out of plane motion (z) to find out that they are identical when the two satellites are flying on a relative projected circular orbit (PCO) and:

$$i_0 = \sin^{-1}\left(\sqrt{\frac{2}{2.5 + \cos^2\alpha}}\right) \tag{6}$$

where α is the initial phase angle along the PCO. According to Eq.(6) the fundamental frequencies can match only at inclinations $i_0 \in [49.11^o, 63.43^o] \cup [116.57^o, 130.89^o]$ when a proper α is selected. Again from Eq.(5) Vadali et al. point out that the amplitude of the out of plane motion can be written as:

$$\frac{\rho_z}{\rho_0} = \sqrt{1 + k^2 t^2 \sin^4 i_0 \cos^2\alpha + kt \sin^2 i_0 \sin 2\alpha} \tag{7}$$

The above equation shows that the out of plane amplitude is zero at $\alpha = 90, 270$ and has no linear growth at $\alpha = 0^o, 180^o$. These conditions, together with Eq.(6), select for the inclination i_0 the values $49.11^o, 130.89^o$ ($\alpha = 0^o, 180^o$) and $63.43^o, 116.57^o$ ($\alpha = 90^o, 270^o$), in perfect accordance to what shown in Figure 1. According to Vadali the magic inclinations are, thus, the only inclinations where the in-plane and out of plane frequencies match and the growth of the out of plane motion of a PCO is contained at the same time.

3. EXPLAINING THE MAGIC: A GENERAL POINT OF VIEW

The explanation of the "*magic inclinations*" (or special inclinations) outlined in Section 2 is based on the hypothesis of small eccentricity ($e \approx 0$), proximity formation flying ($\varphi \approx 0$), PCO relative orbits and J_2 perturbed orbital motion. While perfectly satisfactory in that case, it leaves open the question whether a similar phenomenon can be present for non PCO orbits, in different orbital environments and at significant eccentricity values. According to Wiesel [9], linear systems of differential equations (with time periodic coefficients) can describe the relative satellite motion including higher order harmonics and eccentricity effects up to a high level of detail. Many authors have developed ad hoc linear systems accounting for the sole J_2 effect [10–12] or derived analytical expressions for the transition matrix in many cases.

We will thus here explore the possibility of studying the phenomenon of the "*magic inclinations*" using linear systems. We start in this section by stating a few basic and well-known theorems that will help us later in studying time periodical linear systems.

Consider the following system of ordinary differential equation:

$$\dot{\mathbf{x}} = \mathbf{A}(t)\mathbf{x} \tag{8}$$

where $\mathbf{A}(t+T) = \mathbf{A}(t), \forall t \in R$. The periodicity of the matrix $\mathbf{A}$ is reflected on the solutions of the system as the following theorem shows.

Theorem 1 *If a linear system of homogeneous differential equations with time periodic coefficients of period T admits a periodical solution of period $\tilde{T}$, then necessarily $\tilde{T} = kT, k \in N$*

Proof Let $\mathbf{y}$ be a periodical solution to Eq.(8) and $\tilde{T}$ its period. Then $\mathbf{y}(t) = \mathbf{y}(t+\tilde{T}), \forall t$. As a consequence we get that $\dot{\mathbf{y}}(t) = \dot{\mathbf{y}}(t+\tilde{T})$, which shows how its derivative will also be periodical with the same period. We may express the derivative as follows:

$$\dot{\mathbf{y}}(t) = \mathbf{A}(t)\mathbf{y}(t) = \mathbf{A}(t+\tilde{T})\mathbf{y}(t+\tilde{T}) = \mathbf{A}(t+\tilde{T})\mathbf{y}(t)$$

and we can conclude that, necessarily $\tilde{T} = kT, k \in N$

So if we look for periodical solutions to a system in the form of Eq.(8) we need to look for a kT periodicity, as opposed to what claimed by Bose [13].

Theorem 2 *Eq.(8) has periodical solutions if and only if its transition matrix $\mathbf{\Phi}$ evaluated in T admits the eigenvalue $\lambda = 1$.*

Proof Let $\mathbf{u}$ be the eigenvector associated to the eigenvalue $\lambda = 1$ of the matrix $\mathbf{\Phi}(T)$. Consider the evolution of the system from $\mathbf{u}$. $\mathbf{x}(t) = \mathbf{\Phi}(t)\mathbf{x}(0) \Rightarrow \mathbf{x}(t) = \mathbf{\Phi}(t)\mathbf{u}$. Thus $\mathbf{x}(t+T) = \mathbf{\Phi}(t)\mathbf{\Phi}(T)\mathbf{u} = \mathbf{\Phi}(t)\mathbf{u} = \mathbf{x}(t), \forall t$.

Theorem 3 *If the system in Eq.(8) has one periodical solution, then the whole subspace $\mathcal{S}_k$ spanned by the k eigenvectors associated to the eigenvalue $\lambda = 1$ will result in periodical soultions.*

3.1. Hill's equations

In the case of Hill's equations the transition matrix $\mathbf{\Phi}$ is known in its analytical form and is given, when using non dimensional units, by Eq.(9). We may then evaluate the eigenvalues of this matrix:

$$\lambda_{1,6} = \begin{bmatrix} 1 \\ \cos t + \sqrt{\cos^2 t - 1} \\ \cos t - \sqrt{\cos^2 t - 1} \\ 1 \\ \cos t + \sqrt{\cos^2 t - 1} \\ \cos t - \sqrt{\cos^2 t - 1} \end{bmatrix}$$

At each time instant the eigenvalue $\lambda = 1$ has aritmetic multiplicity equal to at least two. Corresponding to these two eigenvalues there always is only one eigenvector $\mathbf{u} = [0, 1, 0, 0, 0, 0]^T$. This is the leader-follower formation that is an equilibrium point for Hill's equations and thus also a periodical solution for each period t. When $t = \tilde{T} = 2\pi$ the aritmetic multiplicity of the eigenvalue $\lambda = 1$ becomes equal to six. Its geometric multiplicity is, though, only five and in particular the eigenvectors are:

$$\left[\mathbf{u}, \mathbf{u}_a^1, \mathbf{u}_b^1, \mathbf{u}_a^2, \mathbf{u}_b^2\right] = \begin{bmatrix} 1 & 0 & 0 & 0 & 0 \\ 0 & 1 & 0 & 0 & 0 \\ 0 & 0 & 0 & 0 & 1 \\ 0 & 0 & 1 & 0 & 0 \\ -2 & 0 & 0 & 0 & 0 \\ 0 & 0 & 0 & 1 & 0 \end{bmatrix}$$

The five dimensional subspace that results in periodical motion of period $\tilde{T} = 2\pi$ is thus given by the linear combination $\mathbf{x} = k_1\mathbf{u} + k_2\mathbf{u}_a^1 + k_3\mathbf{u}_b^1 + k_4\mathbf{u}_a^2 + k_5\mathbf{u}_b^2$ or equivalently by the condition $x_1 = -2x_5 \rightarrow \delta x = -2\delta\dot{y}$ as well known in this simple case.

4. LINEAR MODELLING

Hill's equations and Tschauner-Hempel equations describe linearly the proximity motion of satellites in perfectly keplerian orbits. The inclusion of orbital perturbations in the linear description of relative satellite motion is the subject of this section, we first give a general framework to derive such equations and then consider the case of the so called J_2 perturbation due to the effect of the planet oblateness [14]. Note that the question of writing linear models for proximity formation flying in the presence of perturbations, is far from trivial and it is a debated problem in modern astrodynamic.

We consider the Chief satellite LHLV reference frame $\mathcal{F}_0$ as our projection frame. Our aim is to derive linear differential equations describing the time evolution of $\delta\mathbf{r}$, the projection in the $\mathcal{F}_0$ frame of the relative position. Consider the simple vectorial equation of motion:

$$\ddot{\vec{\mathbf{r}}} = \vec{\mathbf{g}}(\vec{\mathbf{r}}) + \vec{\mathbf{f}}(\vec{\mathbf{r}})$$

where the gravitational attraction due to a point mass primary is represented by the term $\vec{\mathbf{g}}(\vec{\mathbf{r}})$ and a generic positional perturbation is included in the term $\vec{\mathbf{f}}(\vec{\mathbf{r}})$. Specializing this equation for the Chief and the Deputy we get:

$$\mathbf{\Phi}(t) = \begin{bmatrix} 4-3\cos t & 0 & 0 & \sin t & 2(1-\cos t) & 0 \\ 6(\sin t - t) & 1 & 0 & 2(\cos t - 1) & 4\sin t - 3t & 0 \\ 0 & 0 & \cos t & 0 & 0 & \sin t \\ 3\sin t & 0 & 0 & \cos t & 2\sin t & 0 \\ 6(\cos t - 1) & 0 & 0 & -2\sin t & 4\cos t - 3 & 0 \\ 0 & 0 & -\sin t & 0 & 0 & \cos t \end{bmatrix} \tag{9}$$

Chief As the projection frame is the LHLV frame of the Chief this equation is straight forward:

$$\ddot{\mathbf{r}}_0 + 2\boldsymbol{\omega}_0^{\times}\dot{\mathbf{r}}_0 + \boldsymbol{\omega}_0^{\times}\boldsymbol{\omega}_0^{\times}\dot{\mathbf{r}}_0 + \dot{\boldsymbol{\omega}}_0^{\times}\mathbf{r}_0 = \\ = \mathbf{g}(\mathbf{r}_0) + \mathbf{f}(\mathbf{r}_0)$$

where $\boldsymbol{\omega}$ is the angular velocity of the frame $\mathcal{F}_0$ projected into $\mathcal{F}_0$.

Deputy The equation for the deputy, formally identical, is in reality more complicated as it is projected in the LHLV frame of another satellite: the Chief.

$$\ddot{\mathbf{r}}_1 + 2\boldsymbol{\omega}_0^{\times}\dot{\mathbf{r}}_1 + \boldsymbol{\omega}_0^{\times}\boldsymbol{\omega}_0^{\times}\dot{\mathbf{r}}_1 + \dot{\boldsymbol{\omega}}_0^{\times}\mathbf{r}_1 = \\ = \mathbf{g}(\mathbf{r}_1) + \mathbf{f}(\mathbf{r}_1)$$

Subtracting the two equations and linearizing the forcing terms we get:

$$\ddot{\delta\mathbf{r}} + 2\boldsymbol{\omega}_0^{\times}\dot{\delta\mathbf{r}} + \boldsymbol{\omega}_0^{\times}\boldsymbol{\omega}_0^{\times}\dot{\delta\mathbf{r}} + \dot{\boldsymbol{\omega}}_0^{\times}\delta\mathbf{r} = \\ = \nabla\mathbf{g}(\mathbf{r}_0)\delta\mathbf{r} + \nabla\mathbf{f}(\mathbf{r}_0)\delta\mathbf{r} \tag{10}$$

These equations represent the starting point to derive linear models for the relative motion. Even if formally compact, Eq.(10) can be very complex, depending on the cases. Note that the disturbing terms appear in the right hand side via their gradient, but also in the left hand side via the Chief orbital angular velocity that is influenced by the disturbances.

4.1. The generic LHLV angular velocity $\boldsymbol{\omega}_0$

Here we derive a suitable expression for $\boldsymbol{\omega}_0$ appearing in Eq.(10), that is the projection of the $\mathcal{F}_0$ angular velocity on $\mathcal{F}_0$. Starting from the expression for the Chief orbital angular momentum vector $\vec{\mathbf{h}}_0 = \vec{\mathbf{r}}_0 \wedge \vec{\mathbf{v}}_0$ we project it onto $\mathcal{F}_0$ and obtain:

$$\mathbf{h}_0 = \mathbf{r}_0^{\times}(\dot{\mathbf{r}}_0 + \boldsymbol{\omega}_0^{\times}\mathbf{r}_0) = \mathbf{r}_0^{\times}\boldsymbol{\omega}_0^{\times}\mathbf{r}_0 = r_0^2\boldsymbol{\omega}_0 - (\mathbf{r}_0 \cdot \boldsymbol{\omega}_0)\mathbf{r}_0$$

hence $\boldsymbol{\omega}_0$ has the following expression:

$$\boldsymbol{\omega}_0 = \begin{bmatrix} \omega_{0x} \\ 0 \\ h_0/r_0^2 \end{bmatrix} \tag{11}$$

where an expression for ω_{0x} is still to be found. We take the derivative of the generic orbital angular momentum vector definition $\dot{\vec{\mathbf{h}}}_0 = \vec{\mathbf{r}}_0 \wedge \vec{\mathbf{a}}_0$ and we project it onto $\mathcal{F}_0$ to obtain:

$$\dot{\mathbf{h}}_0 + \boldsymbol{\omega}_0^{\times}\mathbf{h}_0 = \begin{bmatrix} 0 \\ -r_0 f_z \\ r_0 f_y \end{bmatrix}$$

substituting here Eq.(11) and equating the components we have:

$$\dot{h}_0 = r_0 f_y$$
$$\omega_{0x} = r_0/h_0 f_z$$

Thus the expression for $\boldsymbol{\omega}_0$ is:

$$\boldsymbol{\omega}_0 = \begin{bmatrix} r_0/h_0 f_z \\ 0 \\ h_0/r_0^2 \end{bmatrix} \tag{12}$$

and depends, as mentioned above, on the out of plane external perturbation acting on the Chief.

4.2. Expressions for the gradients

A second issue to address when writing explicitly Eq.(10) is that of finding suitable expressions for the gradients $\nabla\mathbf{g}(\mathbf{r}_0)$ and $\nabla\mathbf{f}(\mathbf{r}_0)$. We do not provide here a general treatment of this issue that is formally solved by the established formalism of differentiation in curvilinear coordinates, but we will nevertheless point out that this may not be a trivial calculation. For the term $\nabla\mathbf{g}(\mathbf{r}_0)$ the result is well known and given in Eq.(13)

$$\nabla\mathbf{g}(\mathbf{r}_0) = \frac{\mu}{r_0^3}\begin{bmatrix} 2 & 0 & 0 \\ 0 & -1 & 0 \\ 0 & 0 & -1 \end{bmatrix} \tag{13}$$

As for the expression of $\nabla\mathbf{f}(\mathbf{r}_0)$, a general explicit expression can be given only when the perturbations are specified.

4.3. the J_2 case

In this section we derive the explicit form for Eq.(10) in the case of an external disturbance $\vec{\mathbf{f}}(\vec{\mathbf{r}})$ given by the so called J_2 term of the geopotential field and valid for a Chief orbit with negligible eccentriciy. These equations have been derived by Izzo et al. [11] and compared to other published linear models (in particular to the Schweighart and Sedwick model [10]

recently analysied by Roberts and Roberts [15] and to the Vadali model [12]) by Sabatini et al. [6] revealing to be the most precise tool to describe relative satellite motion in the case considered.

The elements we still need to provide are the orbital radius of the Chief r_0, its orbital momentum h_0 and an expression for the J_2 gradient $\nabla \mathbf{J}_2(\mathbf{r}_0)$. These quantities are all linked to the generic expression for the considered perturbing J_2 force that is [14]:

$$\vec{\mathbf{J}}_2 = -\mathcal{F}^T \frac{K}{4} r_0 \begin{bmatrix} 1 - 3\sin^2 i \sin^2\theta \\ \sin^2 i \sin 2\theta \\ \sin 2i \sin\theta \end{bmatrix} \tag{14}$$

where $K = 6J_2\mu R_E^2/r_0^5$ and $\mathcal{F}$ is the vectrix associated to the LHLV frame of the satellite subject to the disturbing force. The reason to choose this uncommon dimensional group of parameters is linked to the expression of the J_2 gradient

The orbital angular momentum

We start from the expression

$$\dot{h}_0 = r_0 f_y = -\frac{K}{4} r_0^2 \sin^2 i \sin 2\theta_0$$

and we assume $\theta_0 = nt + \theta_i$, $i = i_i$ and $r_0 = r_i$. Note that we make use of this last approximation only to obtain the first order expression for h_0 and not in later derivations. We have:

$$\dot{h}_0 = -\frac{3J_2\mu R_E^2}{2r_i^3} \sin^2 i_i \sin 2\theta_0 \tag{15}$$

Note also that the pedex i refers to the initial state of the Chief, while 0 refers to its instantaneous state. Integrating we get:

$$h_0 = h_i + \frac{3}{4}\mu \frac{J_2 R_E^2}{r_i h_i} \sin^2 i_i (\cos 2\theta_0 - \cos 2\theta_i) \tag{16}$$

where $h_i = \sqrt{\mu r_i}$.

The orbit radius

To evaluate an expression for r_0 we assume that the radius is the sum of a constant keplerian component r_i and a and a time-varying term equal to the along-radius difference between a perturbed and a keplerian orbit. To evaluate this, following the developments in [16], we write the in plane Hill equations perturbed by the J_2 force:

$$\begin{cases} \ddot{\xi} - 2n\dot{\eta} - 3n^2\xi + \frac{K}{4} r_i \left(1 - 3\sin^2 i_i \sin^2\theta_0\right) = 0 \\ \ddot{\eta} + 2n\dot{\xi} + \frac{K}{4} r_i \sin^2 i_i \sin 2\theta_0 = 0 \end{cases}$$

where, again, $\theta_0 = \theta_i + nt$. We solve these equations for the along-track component obtaining:

$$\xi = \frac{3J_2 R_E^2}{2r_i} \left[\frac{1}{3}\sin^2 i_i \cos^2\theta_0 + \frac{1}{3}\sin^2 i_i - 1 + \left(1 - \frac{2}{3}\sin^2 i_i\right)\cos\theta_0\right]$$

We then write the Chief orbit radius

$$r_0 = r_i + \xi \tag{17}$$

and its derivative, useful later when writing down explicitly $\boldsymbol{\omega}_0$

$$\dot{r}_0 = \frac{3J_2 R_E^2}{2r_0} \left[-\frac{1}{3} n \sin^2 i_i \sin 2\theta_0 - n\left(1 - \frac{2}{3}\sin^2 i_i\right)\sin\theta_0\right] \tag{18}$$

The gradient

The general expression for the J_2 gradient is given in [10, 16, 17] and is here reported in Eq.(19), where $K = 6J_2\mu R_E^2/r_0^5$. In using that expression to write down Eq.(10) we will consider $i = i_i$, $\theta_0 = \theta_i + nt$ and $r = r_0$ as given by Eq.(17)

We now have time varying expressions for all the quantities needed to write explicitly Eq.(10):

$$\dot{\mathbf{x}} = \mathbf{A}_{J_2}(t)\mathbf{x} \tag{20}$$

where $\mathbf{x} = [\delta x, \delta y, \delta z, \delta\dot{x}, \delta\dot{y}, \delta\dot{z}]$ and the explicit expressions of the time-varying dynamic matrix are given in the appendix.

5. MAGIC INCLINATONS IN THE LINEAR REGIME

To verify that the linear model is able to reproduce the same behavior of the nonlinear model with respect to the pseudo-periodicity of the relative motion, the same problem of Eq.(1)-(2) is solved numerically using $\mathbf{f}(\mathbf{x}, t) = \mathbf{A}_{J2}(t)\mathbf{x}$

To increase the reliability of the results, two different optimization algorithms are used: a nonlinear programming algorithm - the fmincon MATLAB function - and the same general purpose open source genetic algorithm - PIKAIA, [7] - used in the original study of the nonlinear model [2]. The reference Chief orbit considered has $a_i = 6678$ km, $e_i = 0$, $\theta_i = 0$ and its inclination is considered as a parameter.

The initial point used to initialize the nonlinear optimizer is given by:

$$\mathbf{k}_i = [10^{-9}; 0; 0; 0; 0; 0; T_{kep}]$$

where $T_{kep} = 2\pi/n = 5431$ sec., while it is randomly chosen for the genetic algorithm. The non-zero element $x_i(1)$ is just a numerical expedient to avoid

$$\nabla \mathbf{J}_2(\mathbf{r}_0) = K \begin{bmatrix} 1-3\sin^2 i \sin^2\theta & \sin^2 i \sin 2\theta & \sin 2i \sin\theta \\ \sin^2 i \sin 2\theta & -\frac{1}{4}+\sin^2 i\left(\frac{7}{4}\sin^2\theta-\frac{1}{2}\right) & -\frac{1}{4}\sin 2i\cos\theta \\ \sin 2i \sin\theta & -\frac{1}{4}\sin 2i\cos\theta & -\frac{3}{4}+\sin^2 i\left(\frac{5}{4}\sin^2\theta+\frac{1}{2}\right) \end{bmatrix} \quad (19)$$

singularity in the objective function evaluation. In both cases the the search space has been defined as the hyperectangle $\mathcal{I}_1$ (cf. Section 1) where the units are in km and seconds.

The results are shown in figure 2. The objective function reaches maximum values for two inclinations, namely the magic inclinations 49.1^o and 63.4^o, just like in the nonlinear case (cfr. Figure 1). Note that only a single run of the genetic algorithm has been used in producing Figure 2, which explains the noisy behavior of the graph. We conclude that the linear model here derived is able to capture the phenomenon and can thus be used for its study.

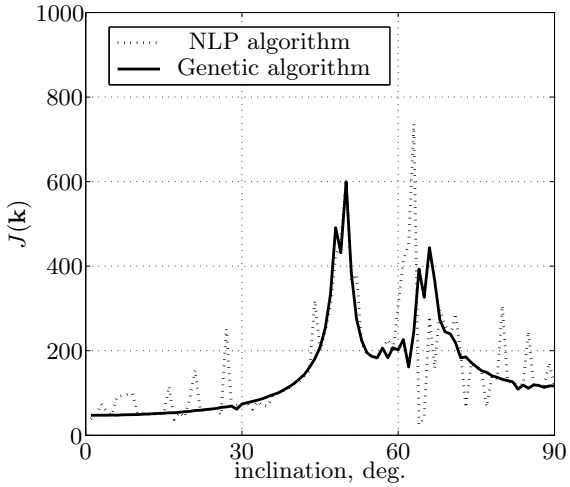

Figure 2. Magic inclinations in the linear model

6. SPECTRAL ANALYSIS OF THE LINEAR MODEL

The time periodic matrix $\mathbf{A}_{J_2}$ is periodic with period T_{kep}, thus, according to the theorems outlined in Section 3 , any time-periodical solution of Eq.(10) must also have period T_{kep} or integer multiples. Writing the solution in terms of its transition matrix helds:

$$\mathbf{x}(t) = \mathbf{\Phi}_{J_2}(t)\mathbf{x}_0$$

applying Theorem 2 to our case we show in Figure 3 a plot of $\det(\mathbf{\Phi}_{J_2}(T_{kep}) - \mathbf{I})$.

We can conclude that there is only one inclination where a purely periodical motion exist, namely 67.77^o. At no other inclination the motion will be

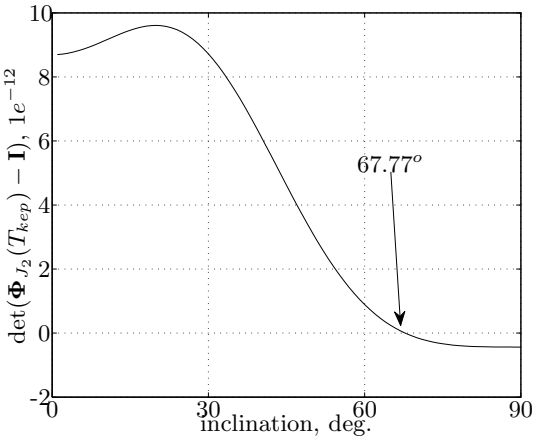

Figure 3. Value of the determinant $\mathbf{\Phi}_{J_2} - \mathbf{I}$ evaluated in $t = T_{kep}$ for different inclinations

periodical. At this unexpected value of the inclination the eigenvalue $\lambda = 1$ has geometrical multiplicity equal to two and its corresponding eigenvectors are

$$\mathbf{u}_{ia} = \begin{bmatrix} -0.00182 \\ 0 \\ 0 \\ 0 \\ 0.0027n \\ 0.99999n \end{bmatrix}, \mathbf{u}_{ib} = \begin{bmatrix} 0 \\ 0.62193 \\ 0.78308 \\ 0.00043n \\ 0 \\ 0 \end{bmatrix}$$

According to Theorem 3, all the initial conditions $\mathbf{x}_i = k_1\mathbf{u}_{ia} + k_2\mathbf{u}_{i_b}$ will result in perfectly periodic motions at this inclination. To support our claim we report, in Figure 4, the result of a 500 orbit propagation of the initial conditions $\mathbf{x}_i = \mathbf{u}_{ib}$. The orbit shown is confirmed to be periodical (in the linear regime), essentially a leader-follower formation with a negligible in-orbit motion. The amplitudes of the z oscillation is comparable to the inter-satellite distance. If we propagate also the initial conditions $\mathbf{x}_i = \mathbf{u}_{ia}$ we obtain another perfectly periodical motion mainly along the z axis, with a negligible in-orbit component.

In order to understand what happens at the other inclination values, and in particular to explain the results obtained solving the optimisation problem stated in Eq.(1) and confirmed by the analysis of Vadali et al. [3], we must weaken our request of periodicity. We will look, in particular, into the possibility to satisfy the relation $\mathbf{x}(T^*) = \mathbf{x}(0)$ for any T^*. This is clearly a necessary condition for periodicity (not sufficient), and would correspond, in the optimisation problem stated by Eqq.(1)-(2), to an objective

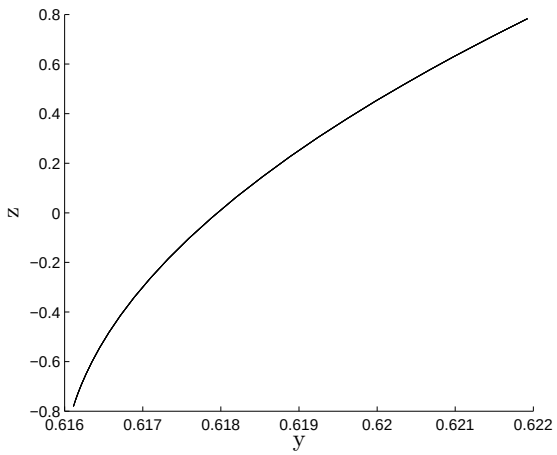

Figure 4. Truly periodic trajectory for the linear model at $i_i = 67.77^o$. (z, y) plane, 500 orbits propagation

function of 1000 (i.e. pseudo-periodic and periodic motions). This condition is satisfied if and only if the equation

$$\det(\mathbf{\Phi}_{J_2}(t) - \mathbf{I}) = 0 \tag{21}$$

admits a solution for at least one $t = T^*$. Such a solution, whenever T^* will be close enough to T_{kep} will result in relative orbits that are not perfectly periodic, but that have nevertheless a very slow drift for a number of initial orbits. Fot this reason we will here refer to those solutions to "*pseudo-periodic*" solutions understanding that this is a definition useful for engineering purposes that does not have a rigorous mathematical character.

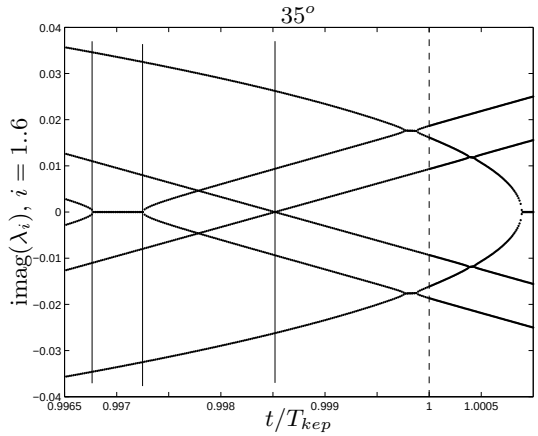

Figure 5. Phase angle for the eigenvalues of $\mathbf{\Phi}$ at $i_i = 35^o$ vs. t/T_{kep}. The vertical lines show time instants where $|\lambda_i| = 1$

To visualise the solutions of Eq.(21) it is useful, given the inclination i_i, to calculate the set of eigenvalues $\lambda_j(t), j = 1..6$ along one entire period. Clearly,

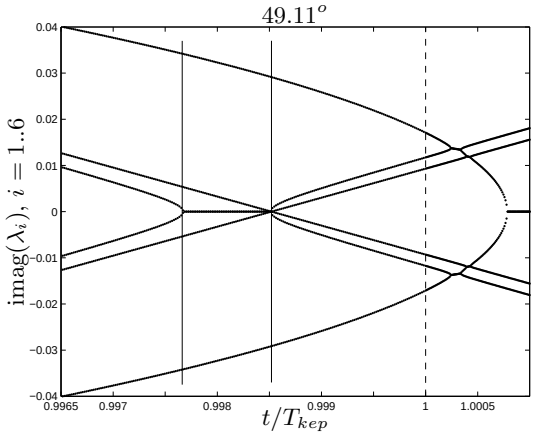

Figure 6. Phase angle for the eigenvalues of $\mathbf{\Phi}$ at $i_i = 49.11^o$ vs. t/T_{kep}. The vertical lines show time instants where $|\lambda_i| = 1$

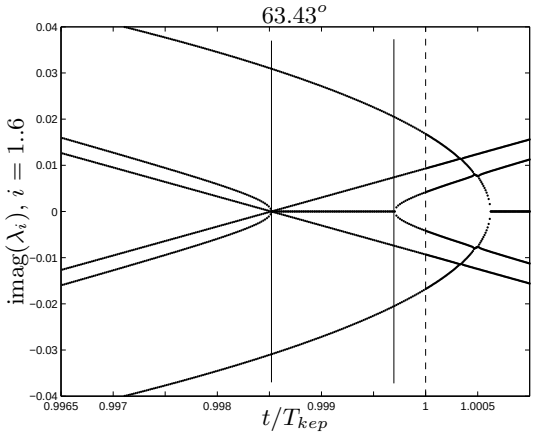

Figure 7. Phase angle for the eigenvalues of $\mathbf{\Phi}$ at $i_i = 63.43^o$ vs. t/T_{kep}. The vertical lines show time instants where $|\lambda_i| = 1$

whenever one of the eigenvalues is equal to one, or equivalently $\mathrm{imag}(\lambda_j) = 0$ and $|\lambda_j| = 1$, Eq.(21) will be verified and a pseudo-periodic orbit will exist. In Figure 5, we have plotted the imaginary part of $\lambda_j(t), j = 1..6$ at $i_i = 35^o$. We also show, with vertical lines, the time locations where $|\lambda_j| = 1$. The seconds around one keplerian period are shown, that is the time interval $5412 - 5436$ sec. in the case of the orbit considered. We note that Eq.(21) is satisfied, in the time interval shown, in three distinct time instants (i.e. $T_1^* = 5413.5$ sec., $T_2^* = 5416.3$ sec. and $T_3^* = 5422.8$ sec.) by two different couples of eigenvectors. A similar situation is found at all values of the inclination i_i except for two remarkable exceptions: the magic inclinations. At these inclinations the situation is that depicted in Figures 6-7. Eq.(21) is again satisfied in two distinct time instants (i.e. $T_1^* = 5418.5$ sec. and $T_2^* = 5422.8$ sec. for $i_i = 49.11^o$ and $T_1^* = 5422.8$ sec. and

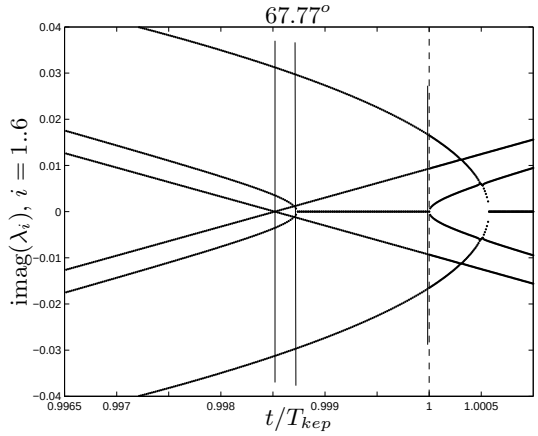

Figure 8. Phase angle for the eigenvalues of $\mathbf{\Phi}$ at $i_i = 67.77^o$ vs. t/T_{kep}. The vertical lines show time instants where $|\lambda_i| = 1$

$T_2^* = 5429.4$ sec. for $i_i = 63.43^o$), but this time at the time $T^* = 5422.8$ sec., there are four eigenvalues that are one, and four corresponding distinct eigenvectors.

A detailed analysis shows that at all inclinations there is one solution fixed at $T^* = 5422.8$ corresponding to the intersection of the cross-shaped eigenvalue lines with the zero axis. The eigenvectors relative to this pseudo periodic motion generate an almost pure in-plane motion. Other solutions are also present and linked to eigenvectors resulting in out of plane motions. At 67.77^o one of these solutions happen at $T^* = T_{kep}$ (cf. Figure 8) allowing for perfectly periodical out of plane motions such as that in Figure 4. Only at the magic inclination values both the out of plane and in plane eigenvectors belong to the same subspace where $\lambda = 1$ thus allowing a great freedom in the design of a pseudo-periodic motion.

7. DISCUSSION

The spectral analysis of the linear model analysis appears to be in contrast with the numerical solution of the optimization problem defined by Eq.(1)-(2). According to paragraph 6 the value $J_{max} = 1000$ can be reached exactly at every inclination value whereas the optimisers manage to find high fitness values only at the magic inclinations (cf. Figure 1 and Figure 2). The reasons are to be found in the dimensions of the space of solutions of Eq.(21). At every inclination it is a bi-dimensional subspace embedded into a seven-dimensional search space (remember that the period is also an optimisation variable). The algorithms used, even if based on completely different approaches (nonlinear programming and genetic), both failed in determining this narrow set of solutions and stopped in local maxima.
On the other hand, for the two magic inclinations, the solution subspace is four-dimensional, thus enhancing the chances for a numerical optimizator to get high fitness values. To confirm that this is indeed the correct explanation, we run again a restricted optimisation limiting the search space to be an in-plane motion: $\mathcal{I}_2 = [-2, 2] \times [-2, 2] \times [-1e-3, 1e-3] \times [-2, 2]n \times [-2, 2]n \times [-1e-3, 1e-3]n \times [T_{kep} - 20, T_{kep} + 20]$ where units are in km and seconds. The results are shown in Figure 9, closing conditions are now detected for a large number of inclinations, though the optimiser still fails to solve the problem at all inclinations.

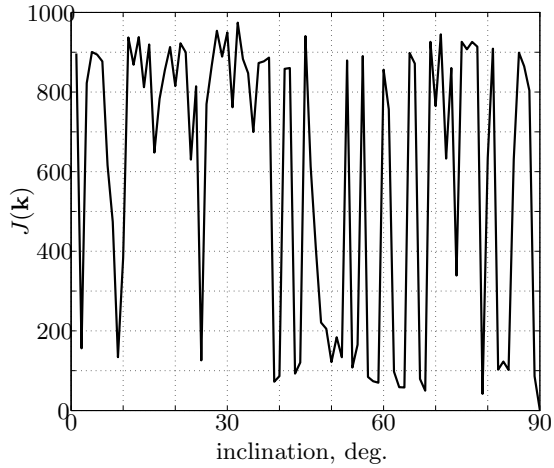

Figure 9. Objective function value for a restricted optimization problem

We now may also explain the results of Vadali et al. [3] who managed to determine analytically the values of the magic inclinations found with a numerical approach in [2]. Vadali demonstration, outlined in Section 2, is restricted to PCO configurations. This kind of relative orbits involves a large motion both in the in-plane and in the out-of-plane directions and this is possible, as explained above, only at the magic inclinations. At other inclination the eigenvectors would result in either an in-plane motion or in an out-of-plane motion.

The initial conditions for PCO orbits can be written as:

$$\mathbf{x}_i = \begin{bmatrix} \rho sin(\alpha)/2 \\ \rho cos(\alpha) \\ \rho sin(\alpha) \\ \rho cos(\alpha)n/2 \\ -\rho sin(\alpha)n \\ \rho cos(\alpha)n \end{bmatrix}$$

To substantiate our claims we run again the non linar programming optimiser using, this time, as initial condition $\mathbf{k}_i = [\mathbf{x}_i, T_{kep}]$ with $\rho = 1$, and as search

space $\mathcal{I}_3 = [-0.1, 0.1] \times [-0.1, 0.1] \times [-0.1, 0.1] \times [-0.1, 0.1]n \times [-0.1, 0.1]n \times [-0.1, 0.1]n \times [T_{kep} - 20, T_{kep} + 20]$ where units are in km and sec. This allow us to look at all inclinations, for pseudo-PCO orbits that satisfy, at least, the necessary condition in Eq.(21).

As expected, only two peaks of the objective function (i.e. only two inclination allowing for pseudo-periodic motion) are found, and these are the first ($i_i = 49.11^o$) and the second ($i_i = 63.43^o$) magic inclination, obtained respectively for $\alpha_0 = 0^o$ and $\alpha_0 = 90^o$, in perfect accordance with Eq.(6) taken from [3].

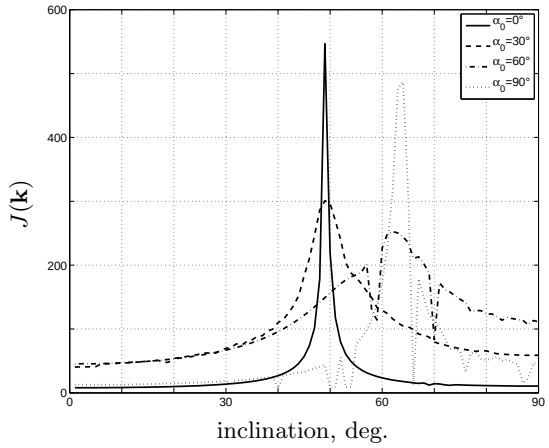

Figure 10. Results of the optimisation for pseudo-PCO relative orbits, according to different initial phase angles

It must be noted that all these considerations are valid for the linear model as well as the nonlinear propagator. In fact, performing the optimisation using a non linear dynamic $\mathbf{f}(\mathbf{x}, t)$ and the same restricted search space $\mathcal{I}_2$ as above, a number of new pseudo-periodical motions are determined (see figure 11).

As a final remark we show, in Figure 12 the non linear propagation (under the J_2 effect) for 20 orbits of the pseudo-PCO orbit (49.11^o) and a normal PCO orbit. We clearly see that without using any control and exploiting natural motion it is possible to obtain (at the magic inclinations values) a pseudo-PCO orbit that remains closed for a remarkable number of orbits and eventually starts drifting away if left uncontrolled. Recently Damarien [18] has produced similar closed orbits at all inclinations forcing the dynamic with a control term.

8. CONCLUSIONS

We showed how the spectral analysis of the linear system representing relative satellite motion sub-

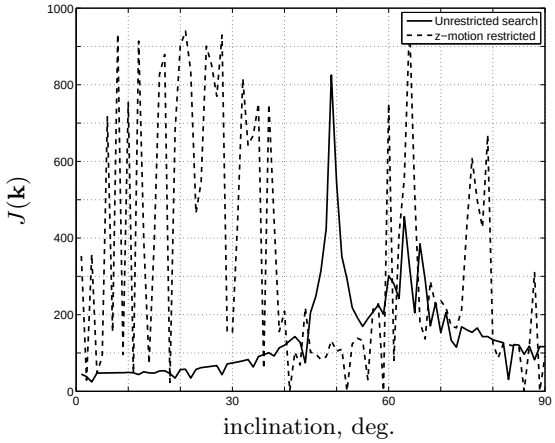

Figure 11. Objective function value for a restricted optimization problem applied to nonlinear system

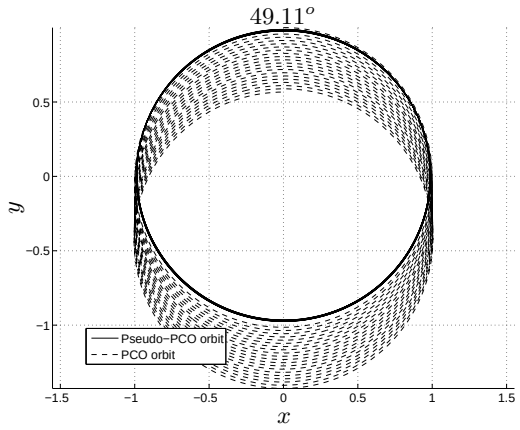

Figure 12. PCO and pseudo-PCO relative orbits. (z, y)plane, 20 periods propagation

ject to the J_2 perturbation explains the recently found peculiarities of the magic (special) inclinations 49.11^o and 63.43^o. These inclinations allow for a pseudo-periodic motion that has both in-plane and out-of-plane components and that results, for example in pseudo-PCO orbits that have a very small orbital drift. We confirmed the utility of the results obtained in the linear regime finding the corresponding phenomena also in the non linear case. We also find that a perfectly periodical motion is possible, in the linear case, only at the inclination value of 67.77^o and mainly as an the out-of-plane motion, and we give an explanation in terms of the spectral properties of the transition matrix.

APPENDIX

Here we report the explicit expressions for the Chief LHLV frame angular velocity $\boldsymbol{\omega}_0$ and the time pe-

riodic matrix $\mathbf{A}$ of the final linear system obtained writing explicitly Eq.(10) in the case of an initially circular Chief orbit subject to the J_2 perturbation. Substituting the third component of Eq.(14) into f_z in Eq.(12) we get:

$$\boldsymbol{\omega}_0 = \begin{bmatrix} -\frac{3}{2} J_2 \mu \frac{R_E^2}{h_0 r_0^3} \sin\theta_0 \sin 2i_i \\ 0 \\ \frac{h_0}{r_0^2} \end{bmatrix}$$

where the expressions for h_0 and r_0 are given, respectively, in Eq.(16) and Eq.(17), and $\theta_0 = \theta_i + nt$. Taking the derivative of this expression we get:

$$\dot{\boldsymbol{\omega}}_0 = \begin{bmatrix} -\frac{3}{2} \frac{J_2 \mu R_E^2}{h_0 r_0^3} \sin 2i_i \left(n\cos\theta_0 - \frac{\dot{h}_0 r_0 + 3 h_0 \dot{r}_0}{h_0 r_0} \sin\theta_0 \right) \\ 0 \\ \frac{\dot{h}_0 r_0 - 2 h_0 \dot{r}_0}{r_0^3} \end{bmatrix}$$

where $\dot{h}_0$ and $\dot{r}_0$ are given respectively, in Eq.(15) and Eq.(18). As for the matrix $\mathbf{A}_{J_2}$ appearing in Eq(20) we have

$$\mathbf{A}_{J_2} = \begin{bmatrix} 0 & 0 & 0 & 1 & 0 & 0 \\ 0 & 0 & 0 & 0 & 1 & 0 \\ 0 & 0 & 0 & 0 & 0 & 1 \\ a_{41} & a_{42} & a_{43} & 0 & 2\omega_{0z} & 0 \\ a_{51} & a_{52} & a_{53} & -2\omega_{0z} & 0 & 2\omega_{0x} \\ a_{61} & a_{62} & a_{63} & 0 & -2\omega_{0x} & 0 \end{bmatrix}$$

where

$$\begin{aligned}
a_{41} &= \omega_{0z}^2 + 2\tfrac{\mu}{r_0^3} + K(1 - 3\sin^2 i_i \sin^2\theta_0) \\
a_{42} &= \dot{\omega}_{0z} + K \sin^2 i_i \sin 2\theta_0 \\
a_{43} &= -\omega_{0x}\omega_{0z} + K \sin 2i_i \sin\theta_0 \\
a_{51} &= -\dot{\omega}_{0z} + K \sin^2 i_i \sin 2\theta_0 \\
a_{52} &= \omega_{0z}^2 + \omega_{0x}^2 - \tfrac{\mu}{r_0^3} + K\left[-\tfrac{1}{4} + \sin^2 i_i \left(\tfrac{7}{4}\sin^2\theta_0 - \tfrac{1}{2}\right)\right] \\
a_{53} &= \dot{\omega}_{0x} - \tfrac{K}{4} \sin 2i_i \cos\theta_0 \\
a_{61} &= -\omega_{0x}\omega_{0z} + K \sin 2i_i \sin\theta_0 \\
a_{62} &= -\dot{\omega}_{0x} - \tfrac{K}{4} \sin 2i_i \cos\theta_0 \\
a_{63} &= \omega_{0x}^2 - \tfrac{\mu}{r_0^3} + K\left[-\tfrac{3}{4} + \sin^2 i_i \left(\tfrac{5}{4}\sin^2\theta_0 + \tfrac{1}{2}\right)\right] \\
K &= \tfrac{6 J_2 \mu R_E^2}{r_0^5} \\
\theta_0 &= \theta_i + nt
\end{aligned}$$

REFERENCES

1. M. Sabatini, R. Bevilacqua, and M. Pantaleoni. A search for invariant relative satellite motion. Technical Report 04-4104a, European Space Agency, the Advanced Concepts Team, 2005. Available on line at www.esa.int/act.

2. M. Sabatini, D. Izzo, and R. Bevilacqua. Special inclinations allowing minimal drift orbits for formation flying satellites. *Journal of Guidance Control and Dynamics*, 31(1):94–100, January-February 2008.

3. S.R. Vadali, P. Sengupta, H. Yan, and Alfriend K.T. On the fundamental frequencies of relative motion and the control of satellite formations. Proceedings of the AAS / AIAA Astrodynamics Specialist Conference, paper AAS 07-427, 2007.

4. M. Sabatini, D. Izzo, and G. Palmerini. Analysis and control of convenient orbital configuration for formation flying missions. Paper AAS 06-120, AAS/AIAA Space Flight Mechanics Conference, Tampa, Florida, 2006.

5. V.M. Becerra, J.D. Biggs, S.J. Nasuto, V.F. Ruiz, W. Holderbaum, and D. Izzo. Using newton's method to search for quasi-periodic relative satellite motion based on nonlinear hamiltonian models. 7th International Conference On Dynamics and Control of Systems and Structures in Space (DCSSS). The Old Royal Naval College, Greenwich, London, England, July 2006.

6. M. Sabatini and G. Palmerini. Linearized formation-flying dynamics in a perturbed orbital environment. 2008.

7. P. Charbonneau. Genetic Algorithms in Astronomy and Astrophysics. *"Astrophysical Journal Supplement"*, 101:309–+, December 1995.

8. P.C. Hughes. *Spacecraft attitude dynamics*. J. Wiley New York, 1986.

9. W.E. Wiesel. Relative satellite motion about an oblate planet. *Journal of Guidance Control and Dynamics*, 25(4):776–785, 2001.

10. S. Schweighart and R. Sedwick. High-fidelity linearized J2 model for satellite formation flight. *Journal of Guidance Control and Dynamics*, 25(6), 2002.

11. D. Izzo, M. Sabatini, and C. Valente. A new linear model describing formation flying dynamics under J2 effect. pages 493–500. Proceedings of the XVII AIDAA congress, 2003.

12. S.R. Vadali, K. Alfriend, and S. Vaddi. Hill's equations, mean orbital elements, and formation flying of satellites. pages 187–203. Texas A&M University/AAS Richard H. Battin Astrodynamics Symp, 2000.

13. A.K. Bose. On the periodic solutions of linear homogeneus systems of differential equations. *Internat. J. Math. & Math. Sci.*, 5(2):305–309, 1981.

14. R.H. Battin. *An Introduction to the Mathematics and Methods of Astrodynamics*. Education Series. AIAA.

15. J.E. Roberts and P.C.E. Roberts. The development of high fidelity linearized J2 models for satellite formation flying control. Paper AAS 04-162, 2004.

16. D. Izzo. Formation Flying for the Mustang Mission. Technical report, Group Design Project, MSc in Astronautics and Space Engineering 2001/02 Cranfield University, 2001.

17. D. Izzo. Formation flying linear modelling. pages 283–289. Proceedings of the 5th International Conference On Dynamics and Control of Systems and Structures in Space, 2002.

18. C. J. Damaren. Almost periodic relative orbits under j2 perturbations. *Proceedings of the I MECH E Part G Journal of Aerospace Engineering*, 221(8):767–774, 2007.